



1 Evaluation and Calibration of a Low-cost Particle Sensor in Ambient 2 Conditions Using Machine Learning Technologies

3 Minxing Si^{1, 2, a}, Xiong Ying^{1, a}, Shan Du³, Ke Du^{1*}

4 ¹Department of Mechanical and Manufacturing Engineering, University of Calgary, 2500 University Drive. NW, Calgary,
5 AB, Canada, T2N 1N4

6 ²Tetra Tech Canada Inc., 140 Quarry Park Blvd, Calgary AB Canada, T2C 3G3

7 ³Department of Computer Science, Lakehead University, 955 Oliver Road, Thunder Bay, ON, Canada, P7B 5E1

8 *Correspondence to Ke Du (kddu@ucalgary.ca)

9 ^aThe authors contributed equally to the work.

10

11 **Abstract.** Particle sensing technology has shown great potential for monitoring particulate matter (PM) with very few
12 temporal and spatial restrictions because of low-cost, compact size, and easy operation. However, the performance of low-
13 cost sensors for PM monitoring in ambient conditions has not been thoroughly evaluated. Monitoring results by low-cost
14 sensors are often questionable. In this study, a low-cost fine particle monitor (Plantower PMS 5003) was co-located with a
15 reference instrument, named Synchronized Hybrid Ambient Real-time Particulate (SHARP) monitor, in Calgary Varsity air
16 monitoring station from December 2018 to April 2019. The study evaluated the performance of this low-cost PM sensor in
17 ambient conditions and calibrated its readings using simple linear regression (SLR), multiple linear regression (MLR), and
18 two more powerful machine learning algorithms using random search techniques for the best model architectures. The two
19 machine learning algorithms are XGBoost and feedforward neural network (NN). Field evaluation showed that the Pearson r
20 between the low-cost sensor and the SHARP instrument was 0.78. Fligner and Killeen (F-K) test indicated a statistically
21 significant difference between the variances of the PM_{2.5} values by the low-cost sensor and by the SHARP instrument. Large
22 overestimations by the low-cost sensor before calibration were observed in the field and were believed to be caused by the
23 variation of ambient relative humidity. The root mean square error (RMSE) was 9.93 when comparing the low-cost sensor
24 with the SHARP instrument. The calibration by the feedforward NN had the smallest RMSE of 3.91 in the test dataset,
25 compared to the calibrations by SLR (4.91), MLR (4.65), and XGBoost (4.19). After calibrations, the F-K test using the test
26 dataset showed that the variances of the PM_{2.5} values by the NN and the XGBoost and by the reference method were not
27 statistically significantly different. From this study, we conclude that feedforward NN is a promising method to address the
28 poor performance of the low-cost sensors for PM_{2.5} monitoring. In addition, the random search method for hyperparameters
29 was demonstrated to be an efficient approach for selecting the best model structure.

30 **Keywords:** Low-cost sensor, machine learning, TensorFlow, XGBoost, PM_{2.5}

31



32 **1 Introduction**

33 Particulate matter (PM), whether it is natural or anthropogenic, has pronounced effects on human health, visibility, and global
34 climate (Charlson et al., 1992; Seinfeld and Pandis, 1998). To minimize the harmful effects of PM pollution, the
35 Government of Canada launched the National Air Pollution Surveillance (NAPS) program in 1969 to monitor and regulate
36 PM and other criteria air pollutants in populated regions, including ozone (O₃), sulfur dioxide (SO₂), carbon monoxide (CO),
37 nitrogen dioxide (NO₂). Currently, PM monitoring is routinely carried out at 286 designated air sampling stations in 203
38 communities in all provinces and territories of Canada (Government of Canada, 2019). Many of the monitoring stations use
39 Beta Attenuation Monitor (BAM), which is based on the adsorption of beta radiation, or Tapered Element Oscillating
40 Microbalance (TEOM) instrument, which is a mass-based technology to measure PM concentrations. An instrument that
41 combines two or more technologies, such as Synchronized Hybrid Ambient Real-time (SHARP), is also used in some
42 monitoring stations. The SHARP instrument combines light scattering with beta attenuation technologies to determine PM
43 concentrations.

44 Although these instruments are believed to be accurate for measuring PM concentration and have been widely used by
45 many air monitoring stations worldwide (Chow and Watson, 1998; Patashnick and Rupprecht, 1991), they have common
46 drawbacks: they can be challenging to operate, bulky, and expensive. The instrument costs from 8,000 Canadian dollars
47 (CAD) to tens of thousands of dollars (Chong and Kumar, 2003). The SHARP instrument used in this study as a reference
48 method costs approximately \$40,000 (CDNova Instrument Ltd., 2017). Significant resources, such as specialized personnel
49 or technicians, are also required for regular system calibration and maintenance. In addition, the sparsely spread stations may
50 only represent PM levels in limited areas near the stations because PM concentrations vary spatially and temporally
51 depending on local emission sources as well as meteorological conditions (Xiong et al., 2017). Such a low-resolution PM
52 monitoring network cannot support public exposure and health effects studies that are related to PM, because these studies
53 require high spatial- and temporal-resolution of monitoring network in the community (Snyder et al., 2013). In addition, the
54 well-characterized scientific PM monitors are not portable due to their large size and volumetric flow rate, which means they
55 are not practical for measuring personal PM exposure (White et al., 2012).

56 As a possible solution to the above problems, a large number of low-cost PM sensors could be deployed, and a high-
57 resolution PM monitoring network could be constructed. Low-cost PM sensors are portable and commercially available.
58 They are cost-effective and easy to deploy, operate, and maintain, which offers significant advantages compared to
59 conventional analytical instruments. If many low-cost sensors are deployed, PM concentrations can be monitored
60 continuously and simultaneously at multiple locations for a reasonable cost (Holstius et al., 2014). A dense monitoring
61 network using low-cost sensors can also assist in mapping hotspots of air pollution, creating emission inventories of air
62 pollutants, and estimating adverse health effects due to personal exposure to the PM (Kumar et al., 2015).



63 However, low-cost sensors present challenges for broad application and installation. Most sensor systems have not been
64 thoroughly evaluated (Williams et al., 2014), and the data generated by these sensors are of questionable quality (Wang et
65 al., 2015). Currently, most low-cost sensors are based on laser light scattering technology (LLS), and the accuracy of LLS is
66 mostly affected by particle composition, size distribution, shape, temperature, and relative humidity (Jayaratne et al., 2018;
67 Wang et al., 2015).

68 Several studies evaluated LLS sensors by comparing the performance of low-cost sensors with medium- to high-cost
69 instruments under laboratory and ambient conditions. For example, Zikova et al. (2017) used low-cost Speck monitors to
70 measure $PM_{2.5}$ concentrations in indoor and outdoor environments, and the low-cost sensors overestimated the concentration
71 by 200% for indoor and 500% for outdoor, compared to a reference instrument – Grimm 1.109 dust monitor. Jayaratne et al.
72 (2018) reported that PM_{10} concentrations generated by a Plantower low-cost particle sensor (PMS 1003) were 46% greater
73 than a TSI 8350 DustTrak DRX aerosol monitor under a foggy environment. Wang et al. (2015) compared PM
74 measurements from three low-cost LLS sensors – Shinyei PPD42NS, Samyoung DSM501A, and Sharp GP2Y1010AU0F –
75 with a SidePack (TSI Inc.) using smoke from burning incense. High linearity was found with R^2 greater than 0.89, but the
76 responses depended on particle composition, size, and humidity. Air Quality Sensor Performance Evaluation Center (AQ-
77 SPEC) of South Coast Air Quality Management District (SCAQMD) also evaluated the performances of three Purple Air
78 PA-II sensors (model: Plantower PMS 5003) by comparing their readings with two United States Environmental Protection
79 Agency (US EPA) Federal Equivalent Method (FEM) instruments – BAM (MetOne) and Grimm dust monitors in laboratory
80 and field environments in south California (Papapostolou et al., 2017). Overall, the three sensors showed moderate to good
81 accuracy, compared to the reference instrument for $PM_{2.5}$ for a concentration range between 0 to $250 \mu g m^{-3}$. Lewis et al.
82 (2016) evaluated low-cost sensors in the field for O_3 , nitrogen oxide (NO), NO_2 , volatile organic compounds (VOCs), $PM_{2.5}$,
83 and PM_{10} ; only O_3 sensors showed good performance compared to the reference measurements.

84 Several studies developed calibration models using multiple techniques to improve low-cost sensors' performance. For
85 example, De Vito et al. (2008) tested feedforward neural network (NN) calibration for benzene monitoring and reported a
86 further calibration was needed for low concentrations. Bayesian optimization was also used to search feedforward NN
87 structures for the calibrations of CO, NO_2 , and NO_x low-cost sensors (De Vito et al., 2009). Zheng et al. (2018) calibrated
88 Plantower low-cost particle sensor PMS 3003 by fitting a linear least-squares regression model. A nonlinear response was
89 observed when ambient $PM_{2.5}$ exceeded $125 \mu g m^{-3}$. The study concluded that a quadratic fit was more appropriate than a
90 linear model to capture this nonlinearity.

91 Zimmerman et al. (2018) explored three different calibration models, including laboratory univariate linear regression,
92 empirical MLR, and a more modern machine learning algorithm, random forests (RF), to improve Real-time Affordable
93 Multiple-Pollutant (RAMP) sensor's performance. They found that the sensors calibrated by RF models improved their
94 accuracy and precision over time, with average relative errors of 14% for CO, 2% for CO_2 , 29% for NO_2 , and 15% for O_3 .



95 The study concluded that combining RF models with low-cost sensors is a promising approach to address the poor
96 performance of low-cost air quality sensors.

97 Spinelle et al. (2015) reported several calibration methods for low-cost O₃ and NO₂ sensors. The best calibration method
98 for NO₂ was an NN algorithm with feedforward architecture. O₃ could be calibrated by simple linear regression (SLR).
99 Spinelle et al. (2017) also evaluated and calibrated NO, CO, and CO₂ sensors, and the calibrations by feedforward NN
100 architectures showed the best results. Similarly, Cordero et al. (2018) performed a two-step calibration for an AQmesh NO₂
101 sensor using supervised machine learning regression algorithms, including NNs, RFs, and Support Vector Machines
102 (SVMs). The first step produced an explanatory variable using multivariate linear regression. In the second step, the
103 explanatory variable was fed into machine learning algorithms, including RF, SVM, and NN. After the calibration, the
104 AQmesh NO₂ sensor met the standards of accuracy for high concentrations of NO₂ in the European Union's Directive
105 2008/50/EC on Air Quality. They highlighted the need to develop an advanced calibration model, especially for each sensor,
106 as the responses of individual sensors are unique.

107 Williams et al. (2014) evaluated eight low-cost PM sensors; the study showed frequent disagreement between the low-
108 cost PM sensors and FEMs. In addition, the study concluded that the performances of the low-cost sensors were significantly
109 impacted by temperature and relative humidity (RH). Recurrent NN architectures were also tested for the calibrations of
110 some gas sensors (De Vito et al., 2018; Esposito et al., 2016). The results showed that the dynamic approaches performed
111 better than traditional static calibration approaches. Calibrations of PM_{2.5} sensors were also reported in recent studies. Lin et
112 al. (2018) performed two-step calibrations for PM_{2.5} sensors using 236 hourly data collected on buses and road cleaning
113 vehicles. The first step was to construct a linear model, and the second step used RF machine learning for further calibration.
114 The RMSE after the calibrations was 14.76 µg m⁻³, compared to a reference method. The reference method used in this study
115 was a Dylos DCI1700 device, which is not a US EPA federal reference method (FRM) or FEM. Loh and Choi (2019) trained
116 and tested SVC, k-nearest neighbor, RF, and XGBoost machine learning algorithms to calibrate PM_{2.5} sensors using 319
117 hourly data. XGBoost archived the best performance with a RMSE of 5.0 µg m⁻³. However, the low-cost sensors in this
118 study were not co-located with the reference method, and the machine learning models were not tested using unseen data
119 (test data) for predictive power and overfitting.

120 Although there are studies in calibrating low-cost sensors, most of them focused on gas sensors or used short-term data to
121 calibrate PM sensors. To our best knowledge, no one has reported studies on PM sensor calibration using random search
122 techniques for the best machine learning model's configuration under ambient conditions during different seasons. In this
123 study, a low-cost fine particle monitor (Plantower PMS 5003) was co-located with a SHARP monitor Model 5030 at Calgary
124 Varsity Air Monitoring Station in an outdoor environment from December 7, 2018, to April 26, 2019. The SHARP
125 instrument is the reference method in this study and is a US EPA FEM (US EPA, 2016). The objectives of this study are:
126 (1) to evaluate the performance of the low-cost PM sensor in a range of outdoor environmental conditions by comparing its



127 PM_{2.5} readings with those obtained from the SHARP instrument; and (2) to assess four calibration methods: a) a SLR or
128 univariate linear regression based on the low-cost sensor values; b) a multiple linear regression (MLR) using the PM_{2.5}, RH,
129 and temperature measured by the low-cost sensor as predictors; c) a decision-tree-based ensemble algorithm, called
130 XGBoost or Extreme Gradient Boosting; and d) a feedforward NN architecture with a backpropagation algorithm.

131 XGBoost and NN are the most popular algorithms used on Kaggle – a platform for data science and machine learning
132 competition. In 2015, 17 winners out of 29 competitions on Kaggle used XGBoost, 11 winners used deep NN algorithm
133 (Chen and Guestrin, 2016).

134 This study is unique in the following ways:

135 1) To the best of our knowledge, this is the first comprehensive study using long-term data to calibrate low-cost
136 particle sensors in the field. Most previous studies focused on calibrating gas sensors (Maag et al., 2018). There are
137 two studies on PM sensor calibrations using machine learning, but they used a short-term dataset that did not
138 include seasonal changes in ambient conditions (Lin et al., 2018; Loh and Choi, 2019). The shortcomings of the two
139 studies were discussed above.

140 2) Although several studies researched the calibration of gas sensors using NN, this study explores multiple
141 hyperparameters to search for the best NN architecture. Previous research configured one to three hyperparameters,
142 compared to six in this study (De Vito et al., 2008, 2009, 2018; Esposito et al., 2016; Spinelle et al., 2015, 2017). In
143 addition, this study tested the Rectified Linear Unit (ReLU) as the activation function in the feedforward NN.
144 Compared to sigmoid and tanh activation functions used in the previous studies for NN calibration models, the
145 ReLU function can accelerate the convergence of stochastic gradient descent to a factor of 6 (Krizhevsky et al.,
146 2017).

147 3) Previous NN and tree-based calibration models used manual search or grid search for hyperparameters tuning. This
148 study introduced random search method for the best calibration models. Random search is more efficient than
149 traditional manual and grid search (Bergstra and Bengio, 2012) and evaluates more of the search space, especially
150 when search space is more than three dimensions (Timbers, 2017).

151 2 Method

152 2.1 Data preparation

153 One low-cost sensor unit was provided by Calgary-based company SensorUp and deployed at the Varsity station in the
154 Calgary Reginal Airshed Zone (CRAZ) in Calgary, Alberta, Canada. The unit contains one sensor, one electrical board, and
155 one housing as a shelter. The sensor in the unit is Plantower PMS 5003, and it measured outdoor fine particle (PM_{2.5})



156 concentrations ($\mu\text{g m}^{-3}$), air temperature ($^{\circ}\text{C}$), and RH (%) every six seconds. The minimum detectable particle diameter by
157 the sensor is $0.3\ \mu\text{m}$. The instrument costs approximately \$20 CAD and is referred to as the low-cost sensor in this paper.

158 The low-cost sensor is based on LLS technology; $\text{PM}_{2.5}$ mass concentration is estimated from the detected amount of
159 scattered light. The LLS sensor is installed on the electrical board and then placed in the shelter for outdoor monitoring. The
160 unit has a wireless link to a router in the Varsity station. A picture of the low-cost sensor and the monitoring environment
161 where the low-cost sensor unit and the SHARP instrument were co-located is provided in Fig. 1. The router uses cellular
162 service to transfer the data from the low-cost sensor to SensorUp's cloud data storage system. The measured outdoor $\text{PM}_{2.5}$,
163 temperature, and RH data at a six-second interval from 00:00 on December 7, 2018, to 23:00 on April 26, 2019, were
164 downloaded from the cloud data storage system for evaluation and calibration.



165
166 **Figure 1:** The low-cost sensor used in the study and the ambient inlet of the reference method – SHARP Model 5030

167 The reference instrument used to evaluate the low-cost sensor is a Thermal Fisher Scientific's SHARP Model 5030. The
168 SHARP instrument was installed at the Calgary Varsity station by CRAZ. The SHARP instrument continuously uses two
169 compatible technologies, light scattering and beta attenuation, to measure $\text{PM}_{2.5}$ every six minutes with an accuracy of $\pm 5\%$.
170 The SHARP instrument is operated and maintained by CRAZ in accordance with the provincial government's guideline
171 outlined in Alberta's air monitoring directive. Hourly $\text{PM}_{2.5}$ data are published on the Alberta Air Data Warehouse website
172 (<http://www.airdata.alberta.ca/>). The Calgary Varsity station also continuously monitors CO, methane, oxides of nitrogen,
173 non-methane hydrocarbons, outdoor air temperature, O_3 , RH, total hydrocarbon, wind direction, and wind speed. Detailed
174 information on the analytical systems for the CRAZ Varsity station can be found on their website
175 (<https://craz.ca/monitoring/info-calgary-nw/>).

176 The ambient conditions in this study measured by the SHARP instrument are presented in Table 1.



177 **Table 1: Ambient Condition Measured by SHARP**

| Climate Data | SHARP Value |
|--------------|----------------------|
| Temperature | -31.4 °C ~ 19 °C |
| RH | 10% ~ 99% |
| Wind Speed | 4.3 ~ 37.1 km/h 10 m |

178

179 The following steps were taken to process the raw data from 00:00 on December 7, 2018, to 23:00 on April 26, 2019:

- 180 1) The six-second interval data recorded by the low-cost sensor, including PM_{2.5}, temperature, and RH, were averaged
181 into hourly data to pair with SHARP data because only hourly SHARP data are publicly available.
- 182 2) The hourly sensor data and hourly SHARP data were combined into one structured data table. PM_{2.5}, temperature,
183 and RH by the low-cost sensor as well as PM_{2.5} by SHARP columns in the data table were selected. The data table
184 then contains 3,384 rows and four columns. Each row represents one hourly data point. The columns include the data
185 measured by the low-cost sensor and the SHARP instrument.
- 186 3) Rows in the data table with missing values were removed – 299 missing values for PM_{2.5} from the low-cost sensor
187 and 36 missing values for PM_{2.5} from the SHARP instrument. The reason for missing data from the SHARP
188 instrument is because of the calibration. However, the reason for missing data from the low-cost sensor is unknown.
- 189 4) The data used for NN were transformed by z standardization with a mean of zero and a standard deviation of one.

190 After the above steps, the processed data table with 3,050 rows and four columns was used for evaluation and calibration.
191 The data file is provided in the supplementary information of this paper. Each row represents one example or sample for the
192 training or testing by the calibration methods.

193 **2.2 Low-cost sensor evaluation**

194 Pearson correlation coefficient was used to compare the correlation for PM_{2.5} values between the low-cost sensor and the
195 SHARP. SHARP was the reference method. The PM_{2.5} data by the low-cost sensor and SHARP were also compared using
196 root mean square error (RMSE), mean square error (MSE), and mean absolute error (MAE).

197 Fligner and Killeen test (F-K test) was used to evaluate the equality (homogeneity) of variances for PM_{2.5} values between
198 the low-cost sensor and the SHARP instrument (Fligner and Killeen, 1976). F-K test is a superior option in terms of
199 robustness and power when data are non-normally distributed, the population means are unknown, or outliers cannot be
200 removed (Conover et al., 1981; de Smith, 2018). The null hypothesis of the F-K test is that all populations' variances are
201 equal; the alternative hypothesis is that the variances are statistically significantly different.



202 2.3 Calibration

203 Four calibration methods were evaluated: SLR, MLR, XGBoost, and NN. Some predictions from the SLR, MLR, and
204 XGBoost have negative values because they extrapolate observed values and regression is unbounded. When the predicted
205 $PM_{2.5}$ values generated by these calibration methods were negative, the negative values were replaced with the sensor data.

206 MLR, XGBoost, and feedforward NN use the $PM_{2.5}$, temperature, and RH data measured by the low-cost sensor as
207 inputs. The $PM_{2.5}$ measured by the SHARP instrument is used as the target to supervise the machine learning process. The
208 processed dataset with 3,050 rows and four columns was randomly shuffled and then divided into a training set, which was
209 the data used to build models and minimize the loss function, and a test set, which was the data that the model has never run
210 with before testing (Si et al., 2019). The test dataset was only used once and gave an unbiased evaluation of the final model's
211 performance. The evaluation was to test the ability of the machine learning model to provide sensible predictions with new
212 inputs (LeCun et al., 2015). The training dataset had 2,440 examples (samples). The test dataset had 610 examples (samples).

213 2.3.1 Simple linear regression and multiple linear regression

214 The calibration by a SLR used Equation 1.

$$215 \hat{y} = \beta_0 + \beta_1 \times PM_{2.5} \quad (1)$$

216 β_0 and β_1 are the model coefficient and were calculated using the training dataset. \hat{y} is model predicted (calibrated) values.
217 $PM_{2.5}$ is the value measured by the low-cost sensor.

218 The MLR used $PM_{2.5}$, RH, and temperature measured by the low-cost sensor as predictors because the low-cost sensor
219 only measured these parameters. The model is expressed as Equation 2.

$$220 \hat{y} = \beta_0 + \beta_1 \times PM_{2.5} + \beta_2 \times T + \beta_3 \times RH \quad (2)$$

221 The model coefficients, β_0 to β_3 , were calculated using the training dataset with SHARP provided readings as \hat{y} . The
222 outputs of the models generated by the SLR and MLR were evaluated by comparing to the SHARP's readings in the test
223 dataset.

224 2.3.2 XGBoost

225 XGBoost is a scalable decision tree-based ensemble algorithm, and it uses a gradient boosting framework (Chen and
226 Guestrin, 2016). The XGBoost was implemented using the XGBoost (Version 0.90) and sklearn (Version 0.21.2) packages
227 in Python (Version 3.7.3). Random search method (Bergstra and Bengio, 2012) was used to tune the hyperparameters in the
228 XGBoost algorithm, and the hyperparameters tuned include

- 229 • Number of trees to fit (`n_estimator`)
- 230 • Maximum depth of a tree (`max_depth`)
- 231 • Step size shrinkage used in update (`learning_rate`)

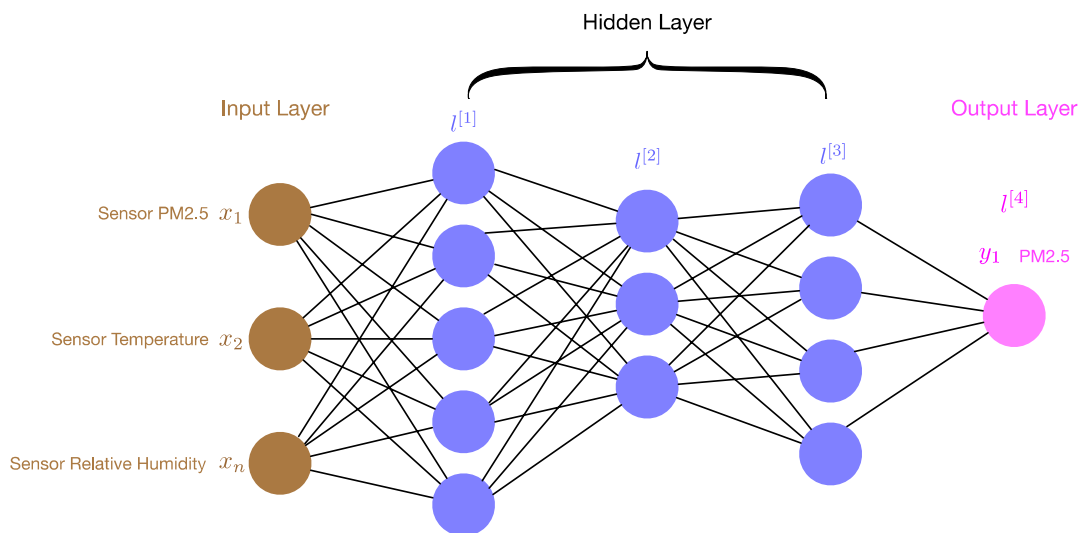


- 232 • Subsample ratio of columns when constructing each tree (colsample_bytree)
233 • Minimum loss reduction required to make a further partition on a leaf node of the tree (gamma)
234 • L2 regularization (Ridge Regression) on weights (reg_lambda)
235 • Minimum sum of instance weight needed in a child (min_child_weight)
236 Ten-fold cross-validation was used to select the best model with minimum MSE from the random search. The best model
237 was then evaluated against the SHARP PM_{2.5} data using the test dataset.

238 2.3.3 Neural network

239 A fully connected feedforward NN architecture was used in the study. In a fully connected NN, each unit (node) in a
240 layer is connected to each unit in the following layer. Data from the input layer are passed through the network until the
241 unit(s) in the output layer is (are) reached. An example of a fully connected feedforward NN is presented in Fig.2. A
242 backpropagation algorithm is used to minimize the difference between the SHARP measured values and the predicted values
243 (Rumelhart et al., 1986).

244



245

246 **Figure 2:** Example of a Neural Network Structure

247 The NN was implemented using the Keras (Version 2.2.4) and TensorFlow (Version 1.14.0) libraries in Python (Version
248 3.7.3). Keras and TensorFlow were the most referenced deep learning framework in scientific research in 2017 (RStudio,
249 2018). Keras is the front end of TensorFlow.



250 Learning rate, L2 regularization rate, numbers of hidden layers, number of units in the hidden layers, and optimization
251 methods were tuned using random search method provided in the scikit-learn machine learning library. Ten-fold cross-
252 validation was used to evaluate the models. The model with the minimum MSE was considered to be the best-fit model and
253 then used for model testing.

254 **3 Results and Discussion**

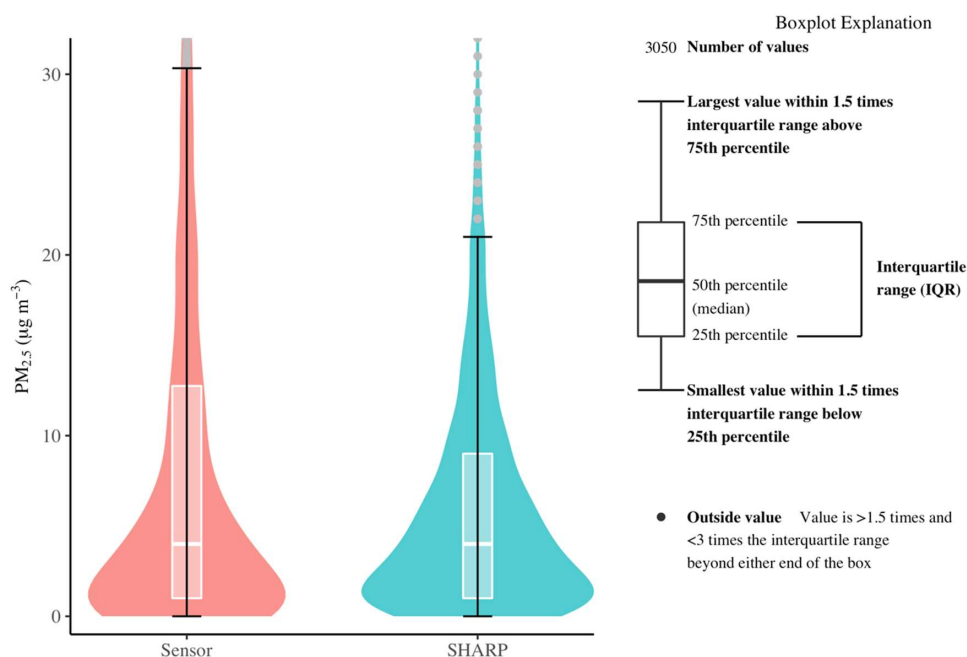
255 **3.1 Sensor evaluation**

256 **3.1.1 Hourly data**

257 The RMSE, MSE, and MAE between the low-cost sensor and SHARP for the hourly $PM_{2.5}$ data were 10.58, 111.83, and
258 5.74. The Pearson correlation coefficient r value was 0.78. The $PM_{2.5}$ concentrations by the sensor ranged from $0 \mu g m^{-3}$ to
259 $178 \mu g m^{-3}$ with a standard deviation of $14.90 \mu g m^{-3}$ and a mean of $9.855 \mu g m^{-3}$. The $PM_{2.5}$ concentrations by SHARP
260 ranged from $0 \mu g m^{-3}$ to $80 \mu g m^{-3}$ with a standard deviation of 7.80 and a mean of $6.55 \mu g m^{-3}$. Both SHARP and the low-
261 cost sensor dataset had a median of $4.00 \mu g m^{-3}$ based on hourly data (Fig.3). The p-value from the F-K test was less than
262 2.2×10^{-16} , indicating that the variance of the $PM_{2.5}$ values measured by the low-cost sensor was statistically significantly
263 different from the variance of the $PM_{2.5}$ values measured by the SHARP instrument.

264

265



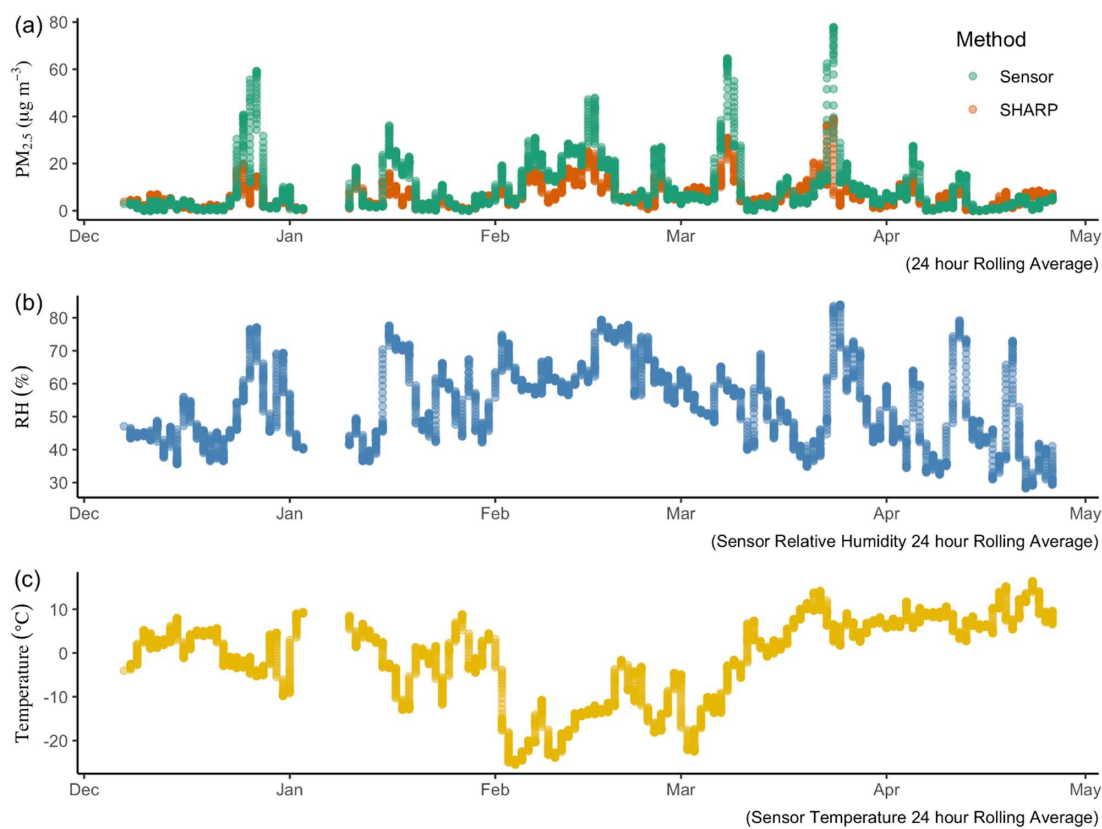
266

267 **Figure 3:** Comparison of the Hourly $PM_{2.5}$ Values between the Low-Cost PM Sensor and SHARP. Based on 3,050 hourly paired data. The
268 low-cost sensor has 250 hourly data greater than $30 \mu\text{g m}^{-3}$. SHARP has 174 hourly data greater than $20 \mu\text{g m}^{-3}$. Bars indicate the 25th and
269 75th percentile values, whiskers extend to values within 1.5 times IQR, and dots represent values outside of the IQR. The boxplot
270 explanation on the right is adjusted from DeCicco (2016)

271 3.1.2 24 Hour rolling average data

272 Over 24 hours, the median value for SHARP was $5.38 \mu\text{g m}^{-3}$ and for the low-cost sensor was $5.01 \mu\text{g m}^{-3}$. Over five months
273 (December 2018 to April 2019), the low-cost sensor tended to generate higher $PM_{2.5}$ values compared to the SHARP
274 monitoring data (Fig. 4)

275

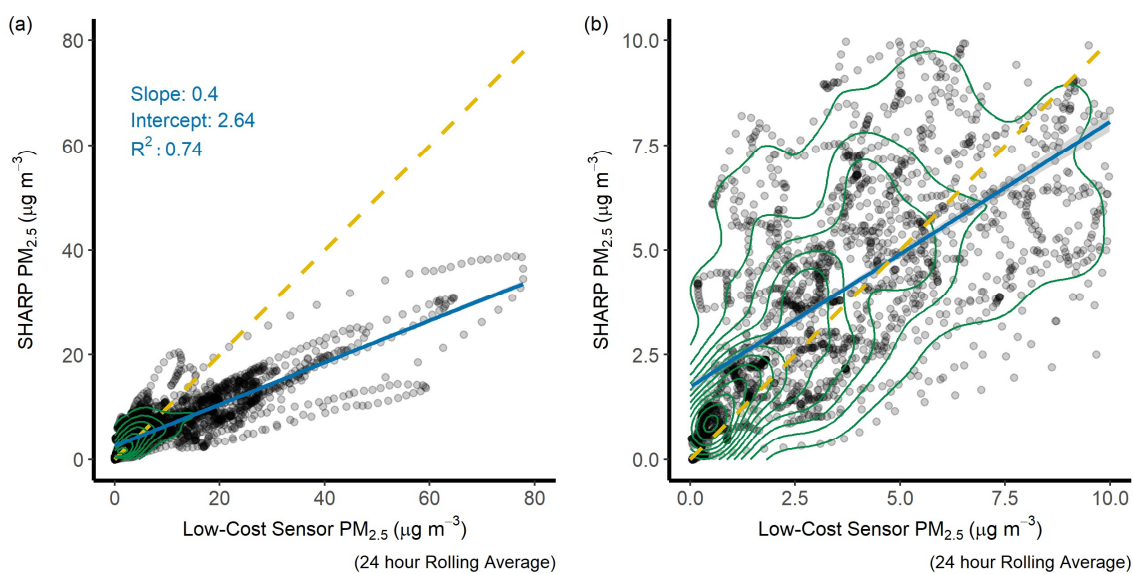


276

277 **Figure 4:** PM_{2.5}, Relative Humidity, and Temperature data on the basis of 24 hour rolling average

278 When PM_{2.5} concentrations were greater than 10 $\mu\text{g m}^{-3}$, the low-cost sensor consistently produced values that were
279 higher than the reference method (Fig.5). When the concentrations were less than 10 $\mu\text{g m}^{-3}$, the performance of the low-cost
280 sensor was closed to the reference method producing slightly smaller values (Fig. 5)

281



282

283 **Figure 5:** SHARP versus Low-Cost Sensor PM_{2.5} Concentration (µg m⁻³). The yellow dashed line is a 1:1 line. The solid blue line is a
 284 regression line. (a) plot is in full scale, (b) plot is a zoom-in plot of plot a. The green circle represents data density.

285 3.2 Calibration by simple linear regression and multiple linear regression

286 The RMSE was 4.91 calibrated by SLR and 4.65 by MLR (Table 2). The r value was 0.74 by the SLR and 0.77 by MLR .
 287 The p-values in the F-K test by the SLR and MRL were less than 0.05, which suggested that the variances of the PM_{2.5}
 288 values were statistically significantly different.

289 **Table 2: Calibration Results by SLR and MLR using Test Dataset**

| Criteria | Low-Cost Sensor | SLR | MLR |
|-------------------------|-------------------------|------------------------|------------------------|
| RMSE | 9.93 | 4.91 | 4.65 |
| MSE | 98.62 | 24.09 | 21.61 |
| MAE | 5.63 | 3.21 | 3.09 |
| Pearson r | 0.74 | 0.74 | 0.77 |
| p-value in the F-K test | 7.062×10^{-09} | 5.81×10^{-13} | 9.90×10^{-10} |
| β_0 | - | 2.49 | 8.47 |
| β_1 | | 0.41 | 0.46 |
| β_2 | | | -0.12 |
| β_3 | | | -0.0055 |

290 Note: The test dataset contains 660 examples.



291 **3.3 Calibration by XGBoost**

292 The hyperparameters selected by the random search for the best model using XGBoost is presented in Table 3.

293 **Table 3: Hyperparameters for the Best XGBoost Model**

| XGBoost Hyperparameters | Values |
|--|---------------|
| Number of trees to fit (n_estimator) | 37 |
| Maximum depth of a tree (max_depth) | 9 |
| Step size shrinkage used in update (learning_rate) | 0.33 |
| Subsample ratio of columns when constructing each tree (colsample_bytree) | 0.83 |
| Minimum loss reduction required to make a further partition on a leaf node of the tree (gamma) | 6.36 |
| L2 regularization (Ridge Regression) on weights (reg_lambda) | 33.08 |
| Minimum sum of instance weight needed in a child (min_child_weight) | 25.53 |

294

295 In the training dataset, the RMSE was 3.03, and the MAE was 1.93 by the best XGBoost model. The RMSE in the test
 296 dataset reduced by 57.8% using the XGBoost from 9.93 by the sensor to 4.19 (Table 4). The p-value in the F-K test using the
 297 test dataset was 0.7256, which showed no evidence that the PM_{2.5} values varied with statistical significance between the
 298 XGBoost predicted values and SHARP measured values.

299 **Table 4: Calibration Results by XGBoost using Test Dataset**

| Criteria | Low-Cost Sensor | XGBoost |
|-------------------------|-------------------------|----------------|
| RMSE | 9.93 | 4.19 |
| MSE | 98.62 | 17.61 |
| MAE | 5.63 | 2.63 |
| Pearson r | 0.74 | 0.82 |
| p-value in the F-K test | 7.062×10^{-09} | 0.7256 |

300 Note: The test dataset contains 610 examples.

301 **3.4 Calibration by neural network**

302 The hyperparameters for the best NN model are presented in Table 5.

303 **Table 5: Hyperparameters for the Best Neural Network Model**

| NN Hyperparameters | Values |
|---|----------------|
| Learning_rate | 0.001 |
| L2 regularization | 0.01 |
| Numbers of hidden layer(s) | 5 |
| Numbers of units in the hidden layer(s) | 32-32-32-32-32 |
| Optimization method | Nadam |



Epochs 100

304

305 In the training dataset, the RMSE was 3.22, and the MAE was 2.17 by the best NN-based model. The RMSE reduced by
306 60% using the NN from 9.93 to 3.91 in the test dataset (Table 6). The p-value in the F-K test was 0.43, which suggested that
307 the variances in the PM_{2.5} values were not statistically significantly different between the NN predicted values and SHARP
308 measured values.

309 **Table 6: Calibration Results by Neural Network using Test Dataset**

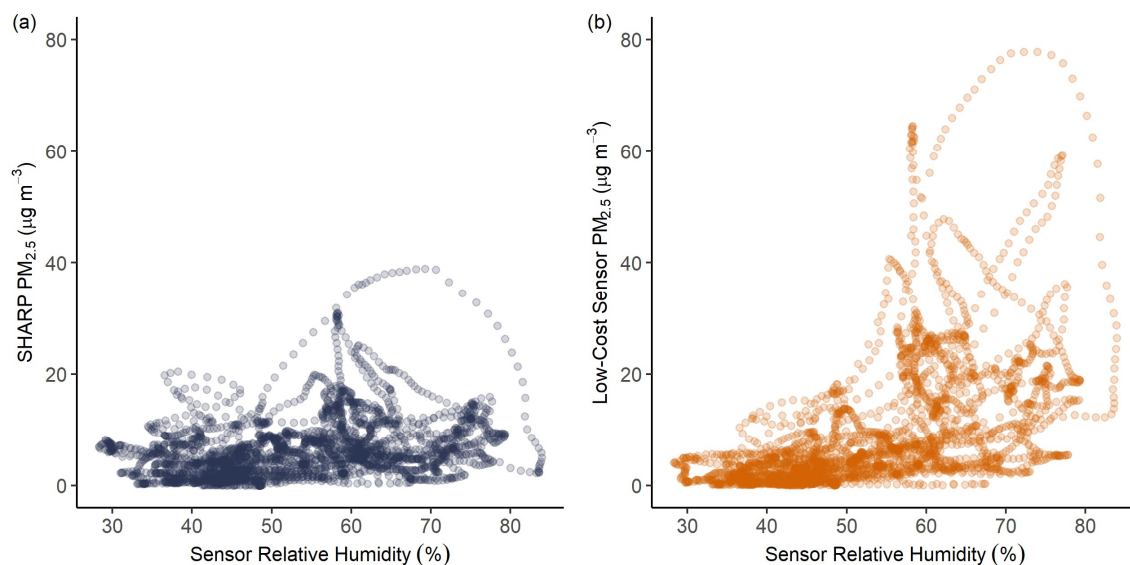
| Criteria | Low-Cost Sensor | Neural Network |
|-------------------------|-------------------------|----------------|
| RMSE | 9.93 | 3.91 |
| MSE | 98.62 | 15.26 |
| MAE | 5.63 | 2.38 |
| Pearson r | 0.74 | 0.85 |
| p-value in the F-K test | 7.062×10^{-09} | 0.43 |

310 Note: the test dataset includes 610 examples.

311 3.5 Discussion

312 3.5.1 Relative humidity impact

313 RH has significant effects on the low-cost sensor's responses. The RH trend matched the low-cost sensor's PM_{2.5} trend
314 closely. The spikes in the low-cost sensor's PM_{2.5} trend corresponded with the increases of RH values, and the low-cost
315 sensor intended to produce inaccurate high PM_{2.5} values when RH suddenly increased (Fig. 4). However, the relationship
316 between PM_{2.5} and RH was not linear (Fig. 6)



317

318 **Figure 6:** PM_{2.5} verse Relative Humidity

319 **3.5.2 Calibration assessment**

320 Descriptive statistics of the PM_{2.5} concentrations in the test dataset for SHARP, low-cost sensor, XGBoost, NN, SLR, and
 321 MLR are presented in Table 7. The arithmetic mean of the PM_{2.5} concentrations measured by the low-cost sensor was
 322 9.44 µg m⁻³. In contrast, the means of the PM_{2.5} concentrations were 6.44 µg m⁻³ by SHARP, 6.40 µg m⁻³ by XGBoost, and
 323 6.09 µg m⁻³ by NN.

324 **Table 7:** Descriptive statistics of PM_{2.5} Concentrations using the Test Dataset

| PM _{2.5} Concentration (µg m ⁻³) | SHARP | Low-Cost Sensor | XGBoost | NN | SLR | MLR |
|---|-------|-----------------|---------|-------|-------|-------|
| Minimum | 0.00 | 0.00 | 0.00 | 0.19 | 2.49 | 0 |
| 1 st quartile | 2.00 | 0.083 | 2.09 | 1.78 | 2.83 | 3.27 |
| Median | 4.00 | 4.00 | 4.98 | 4.16 | 4.13 | 4.79 |
| Mean | 6.44 | 9.44 | 6.40 | 6.09 | 6.37 | 6.42 |
| 3 rd quartile | 8.00 | 11.94 | 8.61 | 8.20 | 7.39 | 7.18 |
| Maximum | 49.00 | 103.33 | 39.94 | 47.19 | 44.97 | 48.56 |



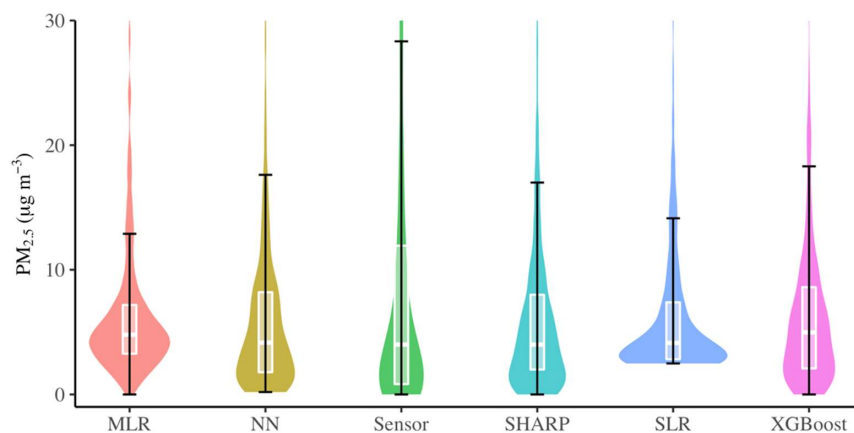
SD 7.32 13.53 6.03 6.23 5.57 5.67

325

326 NN and XGBoost produced data distributions that were similar to SHARP (Fig. 7). SLR had the worst performance.

327 Fig. 7 shows that SLR could not predict low concentrations. The predictions made by NN and XGBoost ranged from

328 $0.19 \mu\text{g m}^{-3}$ to $47.19 \mu\text{g m}^{-3}$ and from $0.00 \mu\text{g m}^{-3}$ to $39.94 \mu\text{g m}^{-3}$.

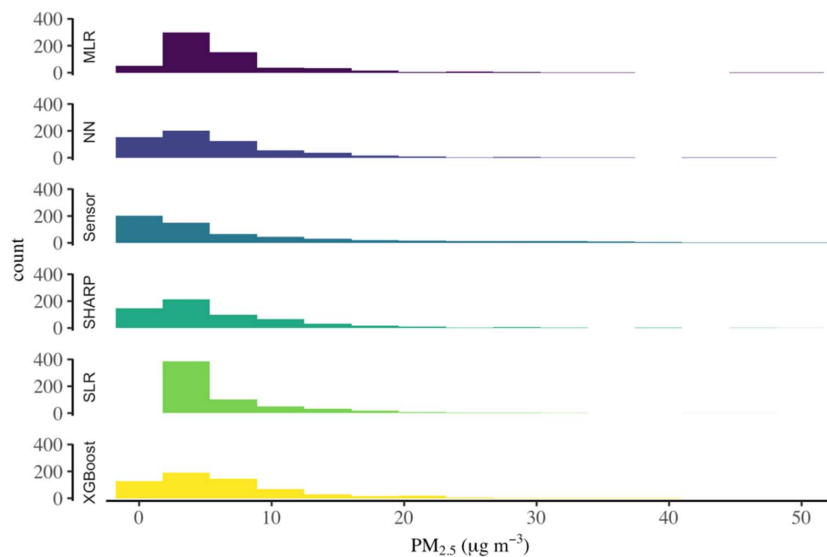


329

330 **Figure 7:** Data Density Comparison in the Test Dataset. Based on 610 Test Examples. NN: neural network, MRL: Multiple Linear
331 Regression, SLR: Simple Linear Regression. $\text{PM}_{2.5}$ data greater than $30 \mu\text{g m}^{-3}$ are not shown in the figure. See the boxplot explanation in
332 Figure 3.

333

334



335

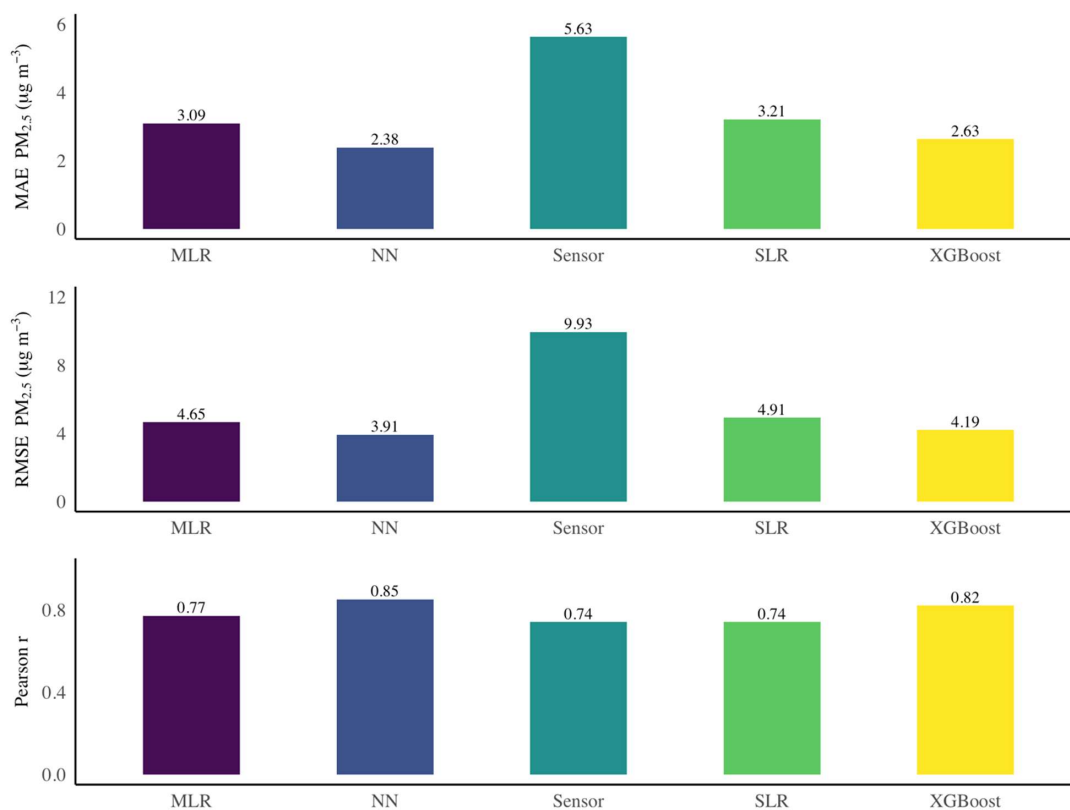
336 **Figure 8:** Data Distribution Comparison. Based on 610 Test Examples. NN: neural network, MRL: Multiple Linear Regression, SLR:
337 Simple Linear Regression.

338

339 In the test dataset, the NN produced the lowest MAE of 2.38 (Fig. 9). The MAEs were 2.63 by XGBoost, 3.09 by MLR,
340 and 3.21 by SLR, when compared with the $PM_{2.5}$ data measured by the SHARP instrument. The NN also had the lowest
341 RMSE score in the test dataset. The RMSEs were 3.91 for the NN, 4.19 for XGBoost, and 9.93 for the low-cost sensor
342 (Fig. 9). The Pearson r value by the NN was 0.85, compared to 0.74 by the low-cost sensor.

343

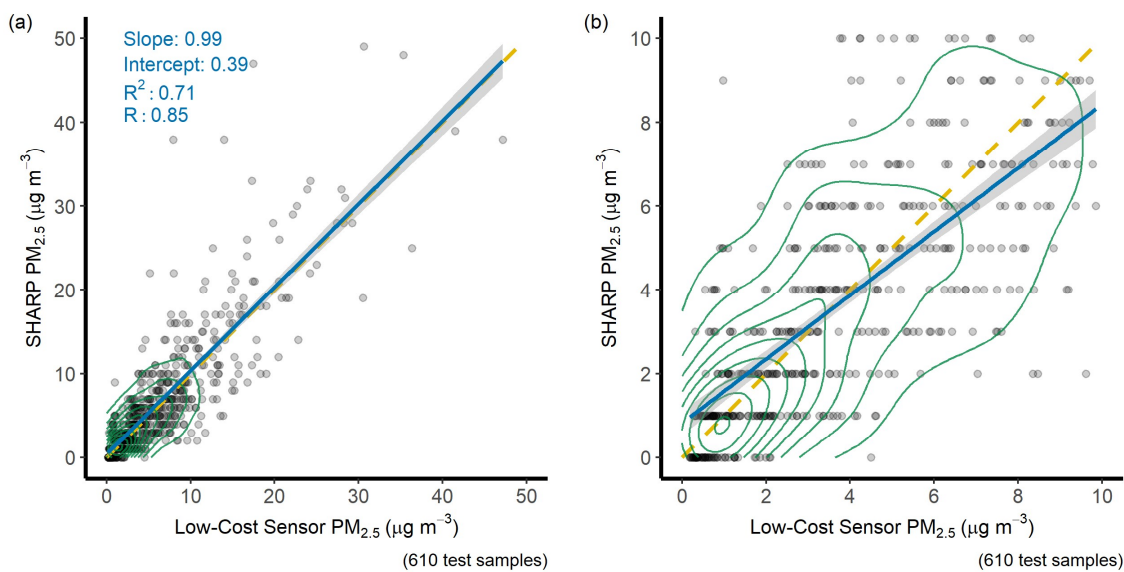
344



345

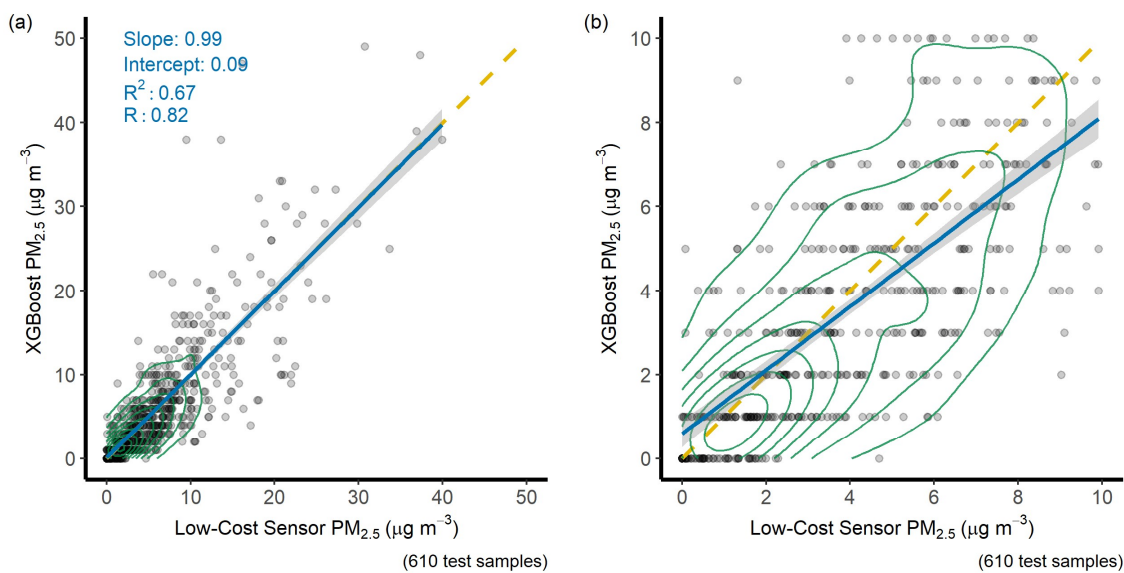
346 **Figure 9:** Performances of Different Calibration Methods. Based on 610 Test Examples. NN: neural network, MRL: Multiple Linear
347 Regression, SLR: Simple Linear Regression.

348 The XGBoost and NN machine learning algorithms have a better performance, compared to traditional SLR and MRL
349 calibration methods. NN calibration reduced RMSE by 60%. Both NN and XGBoost demonstrated the ability to correct the
350 bias for high concentrations made by the low-cost sensor (Fig. 10 and Fig. 11). Most of the values that were greater than
351 $10 \mu\text{g m}^{-3}$ in the NN model fall closer to the yellow 1:1 line (Fig. 10). NN had slightly better performance for low
352 concentrations compared to XGBoost.



353

354 **Figure 10:** Comparison between the NN predictions and SHARP. Based on 610 test examples. Plot (a) is in full scale. Plot (b) is a zoom-
355 in plot of plot (a). The solid blue line is a regression line. The yellow dashed line is a 1:1 line. The green circle represents data density. The
356 grey area along the regression line represents 1 standard deviation.



357



358 **Figure 11:** Comparison between the XGBoost predictions and SHARP. Based on 610 test examples. NN: Neural Network. Plot (a) is in
359 full scale. Plot (b) is a zoom-in plot of plot (a). The solid blue line is a regression line. The yellow dashed line is a 1:1 line. The green
360 circle represents data density. The grey area along the regression line represents 1 standard deviation.

361 4 Conclusions

362 In this study, we evaluated one low-cost sensor against a reference instrument – SHARP – using 3,050 hourly data from
363 00:00 on December 7, 2018, to 23:00 on April 26, 2019. The p-value from the F-K test suggested that the variances in the
364 $PM_{2.5}$ values were statistically significantly different between the low-cost sensor and the SHARP instrument. Based on the
365 24-hour rolling average, the low-cost sensor in this study tended to report higher $PM_{2.5}$ values compared to the SHARP
366 instrument. The low-cost sensor had strong bias when $PM_{2.5}$ concentrations were greater than $10 \mu g m^{-3}$. The study also
367 showed that the sensor's bias responses are likely caused by the sudden changes of RH.

368 Four calibration methods were tested and compared, including SLR, MLR, NN, and XGBoost. The p-values from the
369 F-K tests for the XGBoost and NN were greater than 0.05, which indicated that, after calibration by the XGBoost and the
370 NN, the variances of the $PM_{2.5}$ values were not statistically significantly different from the variance of the $PM_{2.5}$ values
371 measured by the SHARP instrument. In contrast, the p-values from the F-K tests for the SLR and MLR were still less than
372 0.05. The NN generated the lowest RMSE score in the test dataset with 610 samples. The RMSE by NN was 3.91, the lowest
373 of the four methods. RMSEs were 4.91 by SLP, 4.65 by MLR, and 4.19 by XGBoost.

374 However, a wide installation of low-cost sensors may still face challenges, including

- 375 • Durability of low-cost sensor. The low-cost sensor used in the study was deployed in ambient environment. We
376 installed four sensors between December 7, 2018, and June 20, 2019. Only one sensor lasted approximately five
377 months; the data from this sensor was used in this study. The other three sensors only lasted two weeks to one
378 month and collected limited data. These three sensors did not collect enough data for machine learning and,
379 therefore, were not used in this study.
- 380 • Missing data. In this study, the low-cost sensor dataset has 299 missing values for $PM_{2.5}$ concentrations. The reason
381 for the missing data is unknown.
- 382 • Transferability of machine learning models. The models, developed by the two more powerful machine learning
383 algorithms and used to calibrate the low-cost sensor data, tend to be sensor-specific because of the nature of
384 machine learning. Further research is needed to test the transferability of the models for broader use.

385

386

387

388

389



390 *Data availability.* The hourly sensor data and hourly SHARP data are provided online at 10.5281/zenodo.3473833
391
392 *Author Contribution:* MS conducted evaluation and calibrations. YX installed the sensor and monitored and collected the
393 sensor data. MS and YX wrote the manuscript together and have equal contribution. SD edited the machine learning
394 methods. DK secured the funding and supervised the project. All authors discussed the results and commented on the
395 manuscript.
396
397 *Competing interests.* The authors declare no competing interest.
398
399 *Disclaimer.* Reference to any companies or specific commercial products does not constitute endorsement or
400 recommendation by the authors.
401
402 *Acknowledgments.* The authors wish to thank SensorUp for providing the low-cost sensors, and Calgary Region Airshed
403 Zone's air quality program manager Mandeep Dhaliwal for helping with the installation of the PM sensors and a 4G LTE
404 router, as well as the collection of the SHARP data. The authors would also like to thank Jessica Coles for editing this
405 manuscript.
406 The project was funded by Natural Sciences and Engineering Research Council of Canada (NSERC) Engage Program (No.
407 EGP 521823–17) and NSERC Collaborative Research and Development Program (No. CRDPJ 535813-18).

408 **References**

- 409 Bergstra, J. and Bengio, Y.: Random Search for Hyper-Parameter Optimization, *J. Mach. Learn. Res.*, 13, 281–305, 2012.
- 410 CDNova Instrument Ltd.: SHARP Cost Estimate, 2017.
- 411 Charlson, R. J., Schwartz, S. E., Hales, J. M., Cess, R. D., Coakley, J. A., Hansen, J. E. and Hofmann, D. J.: Climate Forcing
412 by Anthropogenic Aerosols, *Science*, 255(5043), 423–430, doi:10.1126/science.255.5043.423, 1992.
- 413 Chen, T. and Guestrin, C.: XGBoost: A Scalable Tree Boosting System, in *Proceedings of the 22nd ACM SIGKDD
414 International Conference on Knowledge Discovery and Data Mining - KDD '16*, pp. 785–794, ACM Press, San Francisco,
415 California, USA., 2016.
- 416 Chong, C.-Y. and Kumar, S. P.: Sensor networks: Evolution, opportunities, and challenges, *Proc. IEEE*, 91(8), 1247–1256,
417 doi:10.1109/JPROC.2003.814918, 2003.
- 418 Chow, J. C. and Watson, J. G.: *Guideline on Speciated Particulate Monitoring*, [online] Available from:
419 <https://www3.epa.gov/ttn/amtic/files/ambient/pm25/spec/drispec.pdf>, 1998.



- 420 Conover, W. J., Johnson, M. E. and Johnson, M. M.: A Comparative Study of Tests for Homogeneity of Variances, with
421 Applications to the Outer Continental Shelf Bidding Data., 1981.
- 422 Cordero, J. M., Borge, R. and Narros, A.: Using statistical methods to carry out in field calibrations of low cost air quality
423 sensors, *Sens. Actuators B Chem.*, 267, 245–254, doi:10.1016/j.snb.2018.04.021, 2018.
- 424 De Vito, S., Massera, E., Piga, M., Martinotto, L. and Di Francia, G.: On field calibration of an electronic nose for benzene
425 estimation in an urban pollution monitoring scenario, *Sens. Actuators B Chem.*, 129(2), 750–757,
426 doi:10.1016/j.snb.2007.09.060, 2008.
- 427 De Vito, S., Piga, M., Martinotto, L. and Di Francia, G.: CO, NO₂, and NO_x urban pollution monitoring with on-field
428 calibrated electronic nose by automatic bayesian regularization, *Sens. Actuators B Chem.*, 143(1), 182–191,
429 doi:10.1016/j.snb.2009.08.041, 2009.
- 430 De Vito, S., Esposito, E., Salvato, M., Popoola, O., Formisano, F., Jones, R. and Di Francia, G.: Calibrating chemical
431 multisensory devices for real world applications: An in-depth comparison of quantitative machine learning approaches, *Sens.*
432 *Actuators B Chem.*, 255, 1191–1210, doi:10.1016/j.snb.2017.07.155, 2018.
- 433 DeCicco, L.: Exploring ggplot2 boxplots - Defining limits and adjusting style, *Explor. Ggplot2 Boxplots - Defini. Limits*
434 *Adjust. Style* [online] Available from: <https://owi.usgs.gov/blog/boxplots/>, 2016.
- 435 Esposito, E., De Vito, S., Salvato, M., Bright, V., Jones, R. L. and Popoola, O.: Dynamic neural network architectures for on
436 field stochastic calibration of indicative low cost air quality sensing systems, *Sens. Actuators B Chem.*, 231, 701–713,
437 doi:10.1016/j.snb.2016.03.038, 2016.
- 438 Fligner, M. A. and Killeen, T. J.: Distribution-Free Two-Sample Tests for Scale, *J. Am. Stat. Assoc.*, 71(353), 210–213,
439 doi:10.1080/01621459.1976.10481517, 1976.
- 440 Government of Canada: National Air Pollution Surveillance (NAPS) Network - Open Government Portal, *Natl. Air Pollut.*
441 *Surveill. NAPS Netw.* [online] Available from: [https://open.canada.ca/data/en/dataset/1b36a356-defd-4813-acea-](https://open.canada.ca/data/en/dataset/1b36a356-defd-4813-acea-47bc3abd859b)
442 [47bc3abd859b](https://open.canada.ca/data/en/dataset/1b36a356-defd-4813-acea-47bc3abd859b) (Accessed 17 September 2019), 2019.
- 443 Holstius, D. M., Pillarisetti, A., Smith, K. R. and Seto, E.: Field calibrations of a low-cost aerosol sensor at a regulatory
444 monitoring site in California, *Atmospheric Meas. Tech.*, 7(4), 1121–1131, doi:10.5194/amt-7-1121-2014, 2014.
- 445 Jayaratne, R., Liu, X., Thai, P., Dunbabin, M. and Morawska, L.: The influence of humidity on the performance of a low-
446 cost air particle mass sensor and the effect of atmospheric fog, *Atmospheric Meas. Tech.*, 11(8), 4883–4890,
447 doi:10.5194/amt-11-4883-2018, 2018.
- 448 Krizhevsky, A., Sutskever, I. and Hinton, G. E.: ImageNet classification with deep convolutional neural networks, *Commun*
449 *ACM*, 60(6), 84–90, 2017.
- 450 Kumar, P., Morawska, L., Martani, C., Biskos, G., Neophytou, M., Di Sabatino, S., Bell, M., Norford, L. and Britter, R.: The
451 rise of low-cost sensing for managing air pollution in cities, *Environ. Int.*, 75, 199–205, doi:10.1016/j.envint.2014.11.019,
452 2015.
- 453 LeCun, Y., Bengio, Y. and Hinton, G.: Deep learning, *Nature*, 521(7553), 436–444, doi:10.1038/nature14539, 2015.



- 454 Lewis, A. C., Lee, J. D., Edwards, P. M., Shaw, M. D., Evans, M. J., Moller, S. J., Smith, K. R., Buckley, J. W., Ellis, M.,
455 Gillot, S. R. and White, A.: Evaluating the performance of low cost chemical sensors for air pollution research, *Faraday*
456 *Discuss.*, 189, 85–103, doi:10.1039/C5FD00201J, 2016.
- 457 Lin, Y., Dong, W. and Chen, Y.: Calibrating Low-Cost Sensors by a Two-Phase Learning Approach for Urban Air Quality
458 Measurement, *Proc. ACM Interact. Mob. Wearable Ubiquitous Technol.*, 2(1), 1–18, doi:10.1145/3191750, 2018.
- 459 Loh, B. G. and Choi, G.-H.: Calibration of Portable Particulate Matter–Monitoring Device using Web Query and Machine
460 Learning, *Saf. Health Work*, S2093791119302811, doi:10.1016/j.shaw.2019.08.002, 2019.
- 461 Maag, B., Zhou, Z. and Thiele, L.: A Survey on Sensor Calibration in Air Pollution Monitoring Deployments, *IEEE Internet*
462 *Things J.*, 5(6), 4857–4870, doi:10.1109/JIOT.2018.2853660, 2018.
- 463 Papapostolou, V., Zhang, H., Feenstra, B. J. and Polidori, A.: Development of an environmental chamber for evaluating the
464 performance of low-cost air quality sensors under controlled conditions, *Atmos. Environ.*, 171, 82–90,
465 doi:10.1016/j.atmosenv.2017.10.003, 2017.
- 466 Patashnick, H. and Rupprecht, E. G.: Continuous PM-10 Measurements Using the Tapered Element Oscillating
467 Microbalance, *J. Air Waste Manag. Assoc.*, 41(8), 1079–1083, doi:10.1080/10473289.1991.10466903, 1991.
- 468 RStudio: Why Use Keras?, [online] Available from: https://keras.rstudio.com/articles/why_use_keras.html, 2018.
- 469 Rumelhart, D. E., Hinton, G. E. and Williams, R. J.: Learning representations by back-propagating errors, *Nature*,
470 323(6088), 533–536, doi:10.1038/323533a0, 1986.
- 471 Seinfeld, J. H. and Pandis, S. N.: *Atmospheric chemistry and physics: from air pollution to climate change*, Wiley, New
472 York., 1998.
- 473 Si, M., Tarnoczi, T. J., Wiens, B. M. and Du, K.: Development of Predictive Emissions Monitoring System Using Open
474 Source Machine Learning Library – Keras: A Case Study on a Cogeneration Unit, *IEEE Access*, 7, 113463–113475,
475 doi:10.1109/ACCESS.2019.2930555, 2019.
- 476 de Smith, M.: *Statistical Analysis Handbook*, 2018 Edition., The Winchelsea Press, Drumlin Security Ltd, Edinburgh.
477 [online] Available from: http://www.statsref.com/HTML/index.html?fligner-killeen_test.html, 2018.
- 478 Snyder, E. G., Watkins, T. H., Solomon, P. A., Thoma, E. D., Williams, R. W., Hagler, G. S. W., Shelow, D., Hindin, D. A.,
479 Kilaru, V. J. and Preuss, P. W.: The Changing Paradigm of Air Pollution Monitoring, *Environ. Sci. Technol.*, 47(20), 11369–
480 11377, doi:10.1021/es4022602, 2013.
- 481 Spinelle, L., Gerboles, M., Villani, M. G., Alexandre, M. and Bonavitacola, F.: Field calibration of a cluster of low-cost
482 available sensors for air quality monitoring. Part A: Ozone and nitrogen dioxide, *Sens. Actuators B Chem.*, 215, 249–257,
483 doi:10.1016/j.snb.2015.03.031, 2015.
- 484 Spinelle, L., Gerboles, M., Villani, M. G., Alexandre, M. and Bonavitacola, F.: Field calibration of a cluster of low-cost
485 commercially available sensors for air quality monitoring. Part B: NO, CO, and CO₂, *Sens. Actuators B Chem.*, 238, 706–
486 715, doi:10.1016/j.snb.2016.07.036, 2017.



- 487 Timbers, F.: Random Search for Hyper-Parameter Optimization | Finbarr Timbers, [online] Available from:
488 <https://finbarr.ca/random-search-hyper-parameter-optimization/> (Accessed 4 October 2019), 2017.
- 489 US EPA: LIST OF DESIGNATED REFERENCE AND EQUIVALENT METHODS, [online] Available from:
490 <https://www3.epa.gov/ttnamti1/files/ambient/criteria/AMTIC%20List%20Dec%202016-2.pdf> (Accessed 7 October 2019),
491 2016.
- 492 Wang, Y., Li, J., Jing, H., Zhang, Q., Jiang, J. and Biswas, P.: Laboratory Evaluation and Calibration of Three Low-Cost
493 Particle Sensors for Particulate Matter Measurement, *Aerosol Sci. Technol.*, 49(11), 1063–1077,
494 doi:10.1080/02786826.2015.1100710, 2015.
- 495 White, R., Paprotny, I., Doering, F., Cascio, W., Solomon, P. and Gundel, L.: Sensors and “apps” for community-based:
496 Atmospheric monitoring, *EM Air Waste Manag. Assoc. Mag. Environ. Manag.*, 36–40, 2012.
- 497 Williams, R., Kaufman, A., Hanley, T., Rice, J. and Garvey, S.: Evaluation of Field-deployed Low Cost PM Sensors, U.S.
498 Environmental Protection Agency. [online] Available from:
499 https://cfpub.epa.gov/si/si_public_record_report.cfm?Lab=NERL&DirEntryId=297517 (Accessed 17 September 2019),
500 2014.
- 501 Xiong, Y., Zhou, J., Schauer, J. J., Yu, W. and Hu, Y.: Seasonal and spatial differences in source contributions to PM_{2.5} in
502 Wuhan, China, *Sci. Total Environ.*, 577, 155–165, doi:10.1016/j.scitotenv.2016.10.150, 2017.
- 503 Zheng, T., Bergin, M. H., Johnson, K. K., Tripathi, S. N., Shirodkar, S., Landis, M. S., Sutaria, R. and Carlson, D. E.: Field
504 evaluation of low-cost particulate matter sensors in high- and low-concentration environments, *Atmospheric Meas. Tech.*,
505 11(8), 4823–4846, doi:10.5194/amt-11-4823-2018, 2018.
- 506 Zikova, N., Hopke, P. K. and Ferro, A. R.: Evaluation of new low-cost particle monitors for PM_{2.5} concentrations
507 measurements, *J. Aerosol Sci.*, 105, 24–34, doi:10.1016/j.jaerosci.2016.11.010, 2017.
- 508 Zimmerman, N., Presto, A. A., Kumar, S. P. N., Gu, J., Hauryliuk, A., Robinson, E. S., Robinson, A. L. and R.
509 Subramanian: A machine learning calibration model using random forests to improve sensor performance for lower-cost air
510 quality monitoring, *Atmospheric Meas. Tech.*, 11(1), 291–313, doi:10.5194/amt-11-291-2018, 2018.

511